



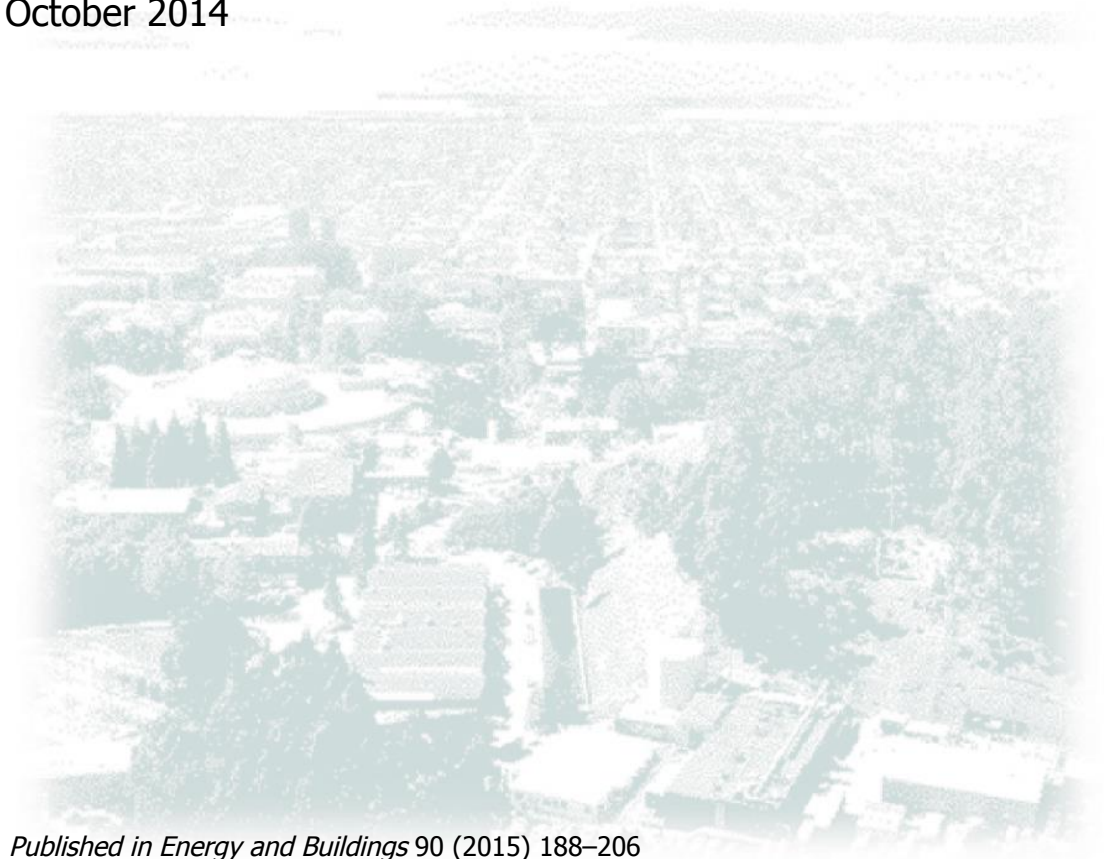
ERNEST ORLANDO LAWRENCE BERKELEY NATIONAL LABORATORY

Angular selective window systems: Assessment of technical potential for energy savings

Luís L. Fernandes, Eleanor S. Lee, Andrew McNeil, Jacob C. Jonsson, Thierry Noudui, Xiufeng Pang, Sabine Hoffmann

Energy Technologies Area

October 2014



Published in Energy and Buildings 90 (2015) 188–206

Disclaimer

This document was prepared as an account of work sponsored by the United States Government. While this document is believed to contain correct information, neither the United States Government nor any agency thereof, nor The Regents of the University of California, nor any of their employees, makes any warranty, express or implied, or assumes any legal responsibility for the accuracy, completeness, or usefulness of any information, apparatus, product, or process disclosed, or represents that its use would not infringe privately owned rights. Reference herein to any specific commercial product, process, or service by its trade name, trademark, manufacturer, or otherwise, does not necessarily constitute or imply its endorsement, recommendation, or favoring by the United States Government or any agency thereof, or The Regents of the University of California. The views and opinions of authors expressed herein do not necessarily state or reflect those of the United States Government or any agency thereof or The Regents of the University of California.

Acknowledgements

We would like to thank and acknowledge our LBNL colleagues for their contribution to this research: Charlie Curcija, Christian Kohler, David Appelfeld, Howdy Goudey, and Robin Mitchell.

This work was supported by the Assistant Secretary for Energy Efficiency and Renewable Energy, Office of Building Technology, State and Community Programs, Office of Building Research and Standards of the U.S. Department of Energy under Contract No. DE-AC02-05CH11231 and by the California Energy Commission through its Public Interest Energy Research (PIER) Program on behalf of the citizens of California.

Angular selective window systems: Assessment of technical potential for energy savings

Luís L. Fernandes¹, Eleanor S. Lee, Andrew McNeil, Jacob C. Jonsson, Thierry Noudui, Xiufeng Pang, Sabine Hoffmann

Building Technologies and Urban Systems Division, Energy Technologies Area, Lawrence Berkeley National Laboratory, Mailstop 90-3111, 1 Cyclotron Road, Berkeley, CA 94720, USA

Abstract

Static angular selective shading systems block direct sunlight and admit daylight within a specific range of incident solar angles. The objective of this study is to quantify their potential to reduce energy use and peak demand in commercial buildings using state-of-the-art whole-building computer simulation software that allows accurate modeling of the behavior of optically-complex fenestration systems such as angular selective systems. Three commercial systems were evaluated: a micro-perforated screen, a tubular shading structure, and an expanded metal mesh. This evaluation was performed through computer simulation for multiple climates (Chicago, Illinois and Houston, Texas), window-to-wall ratios (0.15-0.60), building codes (ASHRAE 90.1-2004 and 2010) and lighting control configurations (with and without). The modeling of the optical complexity of the systems took advantage of the development of state-of-the-art versions of the EnergyPlus, Radiance and Window simulation tools. Results show significant reductions in perimeter zone energy use; the best system reached 28% and 47% savings, respectively without and with daylighting controls (ASHRAE 90.1-2004, south facade, Chicago, WWR=0.45). Angular selectivity and thermal conductance of the angle-selective layer, as well as spectral selectivity of low-emissivity coatings, were identified as factors with significant impact on performance.

Keywords: Building energy-efficiency; daylighting, windows; shading systems; angular selective systems

1. Introduction

1.1 Angular selective shading systems

Static angular selective shading systems block or filter direct sunlight and admit reflected sunlight, diffuse skylight, or ground-reflected daylight within a specific range of incident solar angles [1, 2]. They can be as broadly applicable as non-angular-selective filters, such as diffusing glass, but can deliver potentially more optimal energy efficient performance within the typical 4.6 m (15 ft) deep perimeter zone when tailored to a specific façade orientation and latitude [3].

Angular selective shading systems can be made out of a wide variety of materials, produced in a broad array of shapes, sizes, and colors and are typically located either on the outdoor face of windows or as a between-pane layer in an insulating glass unit (IGU). Commercial products range from woven metal insect screens or punched metal scrims to more engineered systems such as between-pane micro-louvered metal

¹ Corresponding author: Tel.: +1-510-495-8892; Fax: +1-510-486-4089, LLFernandes@lbl.gov.

screens, high-reflectance sculpted meshes or mirrored louver systems. Angular selective coatings on glass [2] are yet another option but are at present not included in this category of technologies.

Arguably, the advantage of such systems is the ability to selectively block direct beam solar radiation, reducing the need for interior shading systems and increasing access to outdoor views. If engineered well, the systems could significantly reduce cooling energy use due to solar heat gains, peak cooling loads, transmission of direct beam irradiation which can cause thermal and visual discomfort, and reduction of window luminance which can cause glare. Exterior punched metal scrims have been used to reduce solar loads [4], enabling all-glass facades to meet energy-efficiency code requirements. Some manufacturers have devised manual and mechanized systems to retract structured panels of these systems when no longer needed. If sufficiently porous to permit wind-induced air flow, exterior shading has also been used with natural ventilation schemes to achieve very low energy use goals [4]. Between-pane systems have the advantage of broader application with potentially longer lifetime durability but cannot be retracted for unobstructed views. These systems must also be designed to avoid damaging low-e coatings during transport or changing optical clarity if off-gassing should occur.

Alternatively, windows with advanced spectrally selective, low emissivity (low-e) coatings are now able to attain very low solar heat gain coefficient (SHGC) levels with high visible transmittance (T_v) (e.g., $SHGC=0.26$, $T_v=0.62$, $K_e=T_v/SHGC=2.38$), but occupants' use of interior shades to block direct sun can significantly reduce useful daylight [5]. Patterned fritted or etched glass has also been used to reduce solar loads, particularly on large-area windows [6]: this has been an architectural trend for at least a decade. This solution also has the disadvantage of not blocking direct beam sunlight, necessitating the need for interior shades in long-term occupied zones.

For most systems, enhancing the distribution of daylight is not intentionally addressed by angular selective shading systems. Most designs diffuse daylight rather than redirect beam sunlight to the building core, but the combination of controlled daylight and reduced need for interior shading can improve daylight availability to building interiors. Reduction in discomfort glare from either direct views of the bright sky or sun orb is possible depending on the optical properties of the shading system; if the system has specular surfaces, localized reflections could increase glare. Unlike attached exterior overhangs or fins where unobstructed views are possible, angular selective shading systems can obscure views out since they are typically designed to cover the entire area of the window. If the shading elements are small, details of the outdoors can still be discerned.

1.2 Computer simulation of optically-complex fenestration

Unlike clear glass or some diffusing materials, angular selective shading systems are optically complex, i.e., they scatter light in ways that are not easily describable by theoretically-derived models or by parametric models fitted to experimental data. An approach that addresses this issue hinges on a discretized bi-directional scattering distribution function (BSDF) [7, 8] that comprehensively describes the scattering of light from an array of directions of incidence spanning an hemisphere to an array of directions of transmission and reflection spanning two hemispheres, one for transmission and another for reflection. The BSDF for a fenestration system can be derived from physical measurements, using a goniophotometer [9], or using computer simulation [10].

Although lighting simulation software, such as Radiance [11, 12, 13] has been able to perform lighting calculations in which the optical properties of materials are determined by BSDF data, the same has not been the case with whole-building simulation software. Programs such as EnergyPlus [14] have used simplified algorithms to determine the transmission of daylight and solar heat gains through fenestration. While these simplified algorithms may be a reasonable approximation for optically-simple fenestration, they most likely fail to capture the complex and highly angle-dependent ways in which optically-complex fenestration systems, and angular selective shading systems in particular, interact with incident radiation.

The approach taken in this paper was to take advantage of experimental, state-of-the-art advances in EnergyPlus that allowed the use of results from highly accurate Radiance simulation instead of EnergyPlus' internal models to more accurately model the optical and near-infrared behavior of angular selective shading systems. This approach was not specific to angular selective shading systems – in fact, its development was intended for any fenestration system that can be modeled by a BSDF. Here, we demonstrate those capabilities in the context of evaluating the technical potential of static angular selective shading systems to reduce energy use and peak demand in commercial buildings.

2. Materials and Methods

The objective of this study is to quantify the technical potential of static angular selective shading systems to reduce energy use and peak demand in commercial buildings. This evaluation of the energy performance of angular selective window systems was performed mainly through computer simulation, thus enabling relatively inexpensive evaluation of several different window systems under a multitude of scenarios, including multiple climates, window-to-wall ratios, building codes and lighting control configurations.

2.1 Materials

Three distinctly different commercial shading systems – an expanded metal mesh, a tubular shading structure, and a micro-perforated screen – were selected for evaluation (Figure 1). Manufacturer center-of-glass specifications of the three systems are shown in Table 1.

2.1.1 Micro-perforated screen

The micro-perforated screen system is marketed as MicroShade by Photosolar A/S. The angular selective micro-perforated screen is applied to the interior surface of the exterior glass pane of an integrated glazing unit (IGU). The two glass panes are clear, the interior pane also having a low emissivity (low-e) coating.

2.1.2 Tubular shading structure

This system consists of a double-glazed IGU filled with plastic tubes, positioned perpendicular to the glass surface. It is marketed as Clearshade IGU by Panelite. When in a two-pane configuration, the interior surface of the exterior glass pane has a pyrolytic low-e coating. This product is available with the plastic tubes in an array of colors. We studied the version with diffuse white plastic tubes. We also studied a three-pane configuration with two low-e coatings.

2.1.3 Expanded metal mesh

The expanded metal mesh system is marketed as Okatech by Okasolar GmbH. The expanded metal mesh layer is mounted inside a triple-glazed IGU, between the exterior and middle panes. There is a low-e coating on the interior surface of the middle pane.

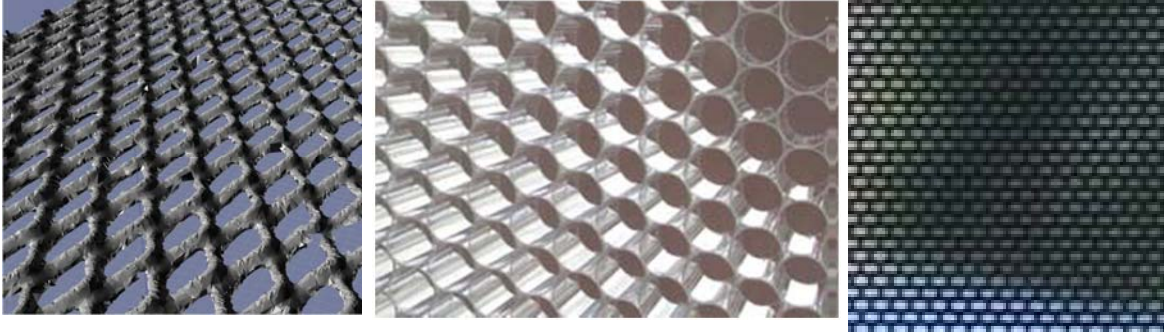


Figure 1. Angular selective shading systems: a) expanded metal mesh (left), b) tubular shading structure (center), and c) micro-perforated screen (right).

Table 1. Manufacturer center-of-glass specifications of the three angular selective shading systems.

	Expanded metal mesh w/ solar control coating		Tubular shading structure (4 TW4)				Microperforated screen (4 MS-A)
U (W/m ² K)	1.0-1.5		1.9				1.1
Angle of incidence (from normal)	0°	60°	45°	50°	60°	70°	0°
Tv	0.26	0.02	n/a	0.24	n/a	0.09	0.49
SHGC	0.18	0.08	0.35	n/a	0.29	0.2	n/a
SC	0.21	0.09	n/a	n/a	n/a	n/a	n/a
Tsol	n/a	n/a	n/a	n/a	n/a	n/a	0.34

2.2 Simulation software

Angular selective shading systems are optically complex and cannot be modeled accurately using conventional simulation tools. State-of-the-art versions of the EnergyPlus, Radiance and Window [15] simulation tools were developed to enable analysis of such systems.

2.2.1 Radiance

Several Radiance programs have been developed to enable the modeling of optically complex fenestration systems (CFS) [11, 12, 13] based on a matrix representation of the propagation of radiation through multilayer windows [7, 8]. *genBSDF* [16] generates bi-directional scattering distribution function (BSDF) data for optically-complex fenestration layers. *genskyvec* generates a vector of sky radiance data according to a predefined discretization of the sky dome [15] (alternate discretizations can be used). *genklemsamp* generates ray origins and directions, according to a predefined hemispherical distribution [15], for use in the generation of matrices of coefficients that describe directional aspects of the propagation of light through environments or materials. *dctimestep* performs matrix calculations using the output of programs like *genBSDF* and *genskyvec*. *dctimestepcpu* is a version of *dctimestep* that is optimized for reducing computation time when performing annual simulations.

2.2.2 Window

A research version of the Window 6 software was developed that can calculate visible and infrared BSDF data for multiple-layer glazing systems [15]. In addition, this software can also output data on the fraction of incident radiation that is absorbed by each window layer, as a function of the angles of incidence.

2.2.3 EnergyPlus

In order to conduct this study, modifications to the EnergyPlus software were made independently (version 6.2) to allow CFS simulation. The modified version contains two main changes from the standard version: it allows the use of schedules for a) interior surface heat gains from windows and b) radiation absorption by window layers. This means that the values for these quantities that are calculated internally by EnergyPlus are disregarded in favor of the values provided by external schedule files². These files are generated prior to the EnergyPlus runs using Radiance, allowing significantly more accurate modeling of both propagation of radiation through CFS (including layer absorption) and the distribution of transmitted radiation throughout the interior space.

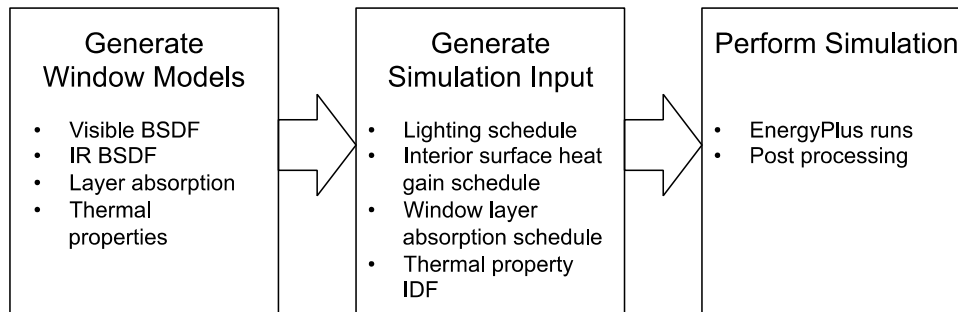


Figure 2. Simulation workflow.

2.3 Simulation workflow

The simulations were conducted in three broad steps (Figure 2). First, models of the bi-directional optical properties of the angular selective systems were developed. Second, these models were used to generate lighting, interior surface gain and window layer absorption schedules for input into EnergyPlus. Finally, whole-building annual energy simulations were conducted using EnergyPlus.

2.3.1 Window models

Visible and infrared BSDF properties of the materials of which each angular selective layer was made were measured using a goniophotometer, as in [9]. These material properties, as well as the geometry of the layer, were then used to develop a Radiance model of the geometry of the layer. In the case of the expanded metal mesh, samples of the material were not available, and the layer BSDF was determined via parametric simulation comparing *genBSDF* results to whole layer goniophotometer measurements [10]. The geometry of the tubular shading structure was easily describable in Radiance using parameters. A Radiance description of the more complex geometry of the microperforated screen was developed based on manufacturer drawings [17]. For the expanded metal mesh system, in the absence of detailed geometry information, a description was obtained using a coordinate measuring machine (Figure 3). Layer BSDF was generated with *genBSDF* and input into Window 6 as a shading layer. A model for the whole glazing was then built in Window 6, according to each system's published specifications. Output was in the form of visible/infrared BSDF data for the whole window, and angle-dependent absorption for each layer. Window 6 also output a description of the physical dimensions, construction and thermal properties of the window in EnergyPlus input format (IDF).

² This extension of the standard capabilities of the EnergyPlus schedule object has since been incorporated into an official EnergyPlus release.



Figure 3. Scanning of expanded metal mesh layer using coordinate measuring machine.

2.3.2 EnergyPlus input files

Visible BSDF data was input into Radiance programs *dctimestepcpu*, *genskyvec*, and *genklemsamp* in order to determine interior daylight levels for each time step, and then the amount of electric lighting necessary to maintain the lighting setpoint of 500 lux. This was then converted into an EnergyPlus lighting schedule. A similar procedure took place using IR BSDF data to determine the amount of radiation reaching each interior wall, floor and ceiling surface (radiation hitting furniture was included in the floor radiation), assuming a surface solar absorptance of 100%, which was then converted into an EnergyPlus schedule for interior surface heat gains. A schedule for window layer absorption of radiation was created using the angle-dependent Window 6 output. Together with the window property IDF file, this data was assembled into a complete EnergyPlus input file for each building model, location, window system, window-to-wall ratio, and lighting controls configuration.

2.3.3 EnergyPlus simulation

Annual energy simulation runs were performed for each simulation using EnergyPlus version 6.2 with the modifications mentioned in the previous subsection, in a Linux cluster computer with 158 nodes, each having two Xeon Intel hex-core 64-bit Westmere processors. A single simulation, including schedule generation, took approximately 2 hours using a single CPU. To make the full energy impacts of windows discernible, hourly output was post-processed to allocate HVAC plant (boiler and chiller) and system (air handling unit) energy consumption between core and perimeter zones, for each façade orientation.

2.4 Building model

Simulations were conducted using the DOE large office commercial reference building model [18]. These models provide a common starting point to measure progress toward DOE energy efficiency goals and are meant to represent both new and existing buildings. The models were derived from the 2003 CBECS standards for building types, and experience with commercial buildings. They are hypothetical with ideal operations that meet certain minimum requirements. These models were further modified as part of DOE's Advanced Codes Initiative to produce code-compliant models for each version of Standard 90.1, known as the 90.1 prototype building models.

For the purposes of this study, the DOE model was modified so that perimeter zones were separated from the core. This was important because the impact of window systems on energy consumption is much greater in perimeter zones than in the core of buildings.

In addition to glazing type, several other simulation parameters were also varied (Table 2): building code, location, window-to-wall ratio (WWR), daylighting controls. Two building codes were used, ASHRAE

90.1-2004 and 2010. The first represented typical buildings in the United States, whereas the second represented more recent construction. Chicago and Houston were used as locations, the first with significant heating and cooling seasons, and the second almost entirely cooling-dominated. Window-to-wall ratio was varied from 0.15 to 0.6, with 0.3 and 0.45 as intermediate steps. Simulations were performed with and without daylighting controls.

Table 2. Simulation parameters

Parameter	Values
Climate	Chicago, Houston
Building code	ASHRAE 90.1-2004, 2010
WWR	0.15, 0.3, 0.45, 0.6
Daylighting controls	None, Continuous dimming

The modeled building was twelve stories high (Figure 4), with a total floor area of approximately 46,378 m² (499,207 ft²). Each floor was zoned as shown in Figure 4, with the façade subdivided every 12.2 m (40 ft). Perimeter zones were 4.6 m (15 ft) deep, and core zones 10.1 m (33 ft). Each zone was modeled with standard office furniture (Figure 5). Floor area per occupant was 18.6 m² (200 ft²). No exterior obstructions were considered. Plug and process load density was 8.07 W/m² (0.75 W/ft²) and lighting power density was 10.76 W/m² (1.00 W/ft²) in the 2004 model and 9.00 W/m² (0.84 W/ft²) in the 2010 model.

The three angular selective windows were modeled with the composition shown in Table 3. Frame thermal properties are shown in Table 4 and cross-section in Figure 6. Center of glass solar-optical and thermal properties are shown in Table 5. The composition of these models was based on the manufacturers' specifications as well as on measurements of the geometry, optical and thermal properties of the angular selective layers. In addition to the angular selective systems, and to enable benchmarking of their performance, an array of other types of windows were modeled (see list in Table 6): a) code-compliant windows for each of the climate/code configurations; b) double- and triple-pane windows with highly spectrally selective low-e coatings, with and without interior shading or exterior blinds; c) versions of the angular selective systems with exterior or interior shading, or with the angular selective layer mounted outside the glazing; d) versions of the angular selective systems without the angular selective layer, and/or without the inert gas fill, and/or without the low-e coatings; e) versions of the angular selective systems with an invariant IGU construction, i.e. varying the angular selective layer only.

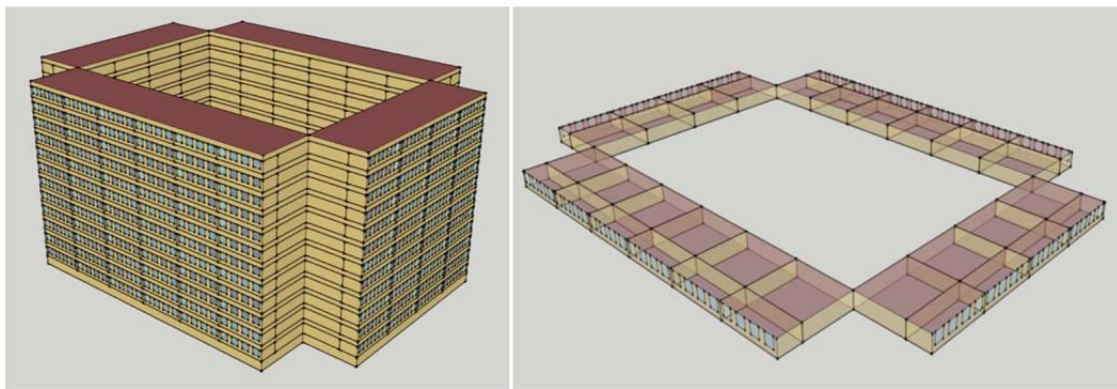


Figure 4. Building model and floor geometry.

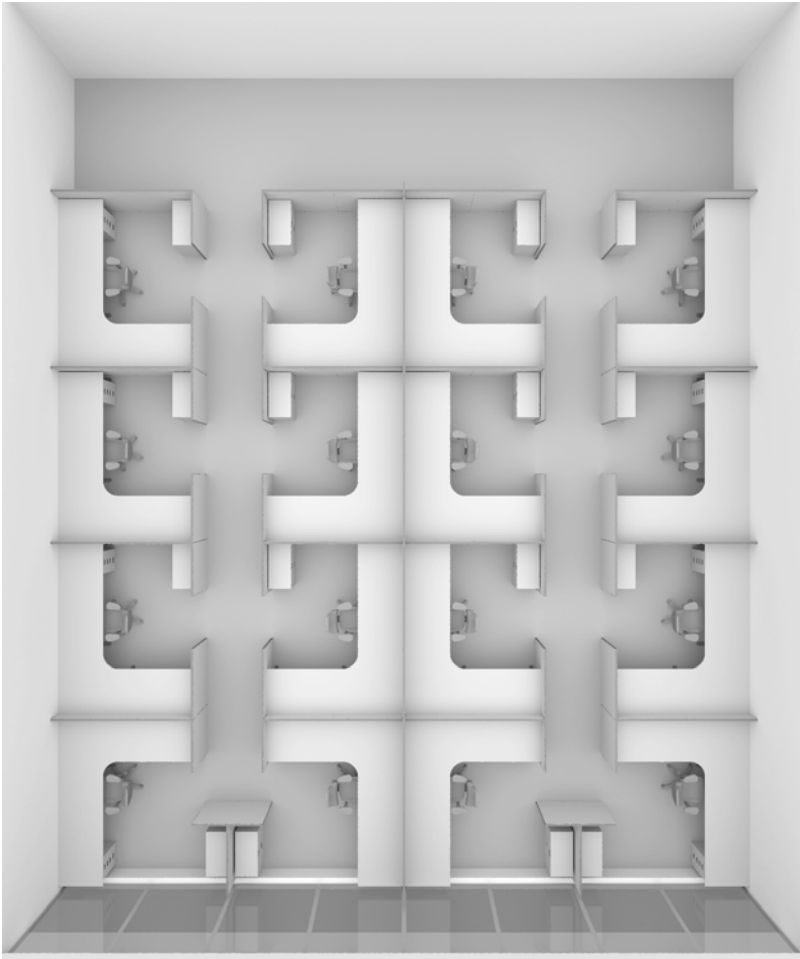


Figure 5. Furniture layout in a perimeter zone.

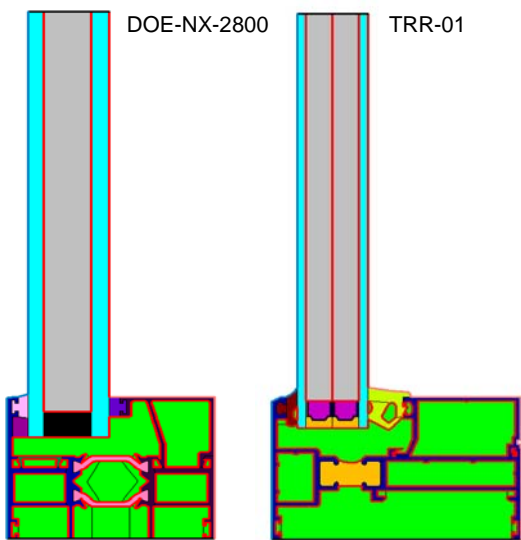


Figure 6. Cross-sectional diagrams of the two frame types.

Table 3. Angular selective window composition.

Window	Framing	Layers (outside to inside)
Microperforated screen	TRR-01	Clear glass 6 mm
		Argon mix fill 0.1 mm
		Microshade microperforated screen
		Argon mix fill 12.7 mm
		PPG Solarban 70XL on Starphire 6 mm
Tubular shading structure (double pane)	TRR-01	PPG Sungate 500 on Clear
		Argon mix fill 0.1 mm
		Panelite tubular shading structure
		Argon mix fill 0.1 mm
		Clear glass 6 mm
Tubular shading structure (triple pane)	TRR-01	Clear glass 6 mm
		Argon mix fill 0.1 mm
		Panelite tubular shading structure
		Argon mix fill 0.1 mm
		PPG Solarban 70XL on Starphire 6 mm
		Argon mix fill 12.7 mm
		PPG Solarban 70XL on Starphire 6 mm
Expanded metal mesh	DOE-NX-2800	Clear glass 6 mm
		Argon mix fill 0.1 mm
		Okatech expanded metal mesh
		Argon mix fill 0.1 mm
		PPG Solarban 70XL on Clear 3 mm
		Argon mix fill 12.7 mm
		Clear glass 6 mm

Table 4. Thermal properties of the two window frame types.

Name	Part	U _{val} W/(m ² ·K)	U _{edge} W/(m ² ·K)
DOE-NX-2800	Head	2.842	1.832
	Jamb	2.800	1.826
	Sill	2.815	1.826
TRR-01	Head	5.149	1.646
	Jamb	5.456	1.646
	Sill	5.148	1.646

Table 5. Center of glass solar-optical and thermal properties of the angular selective window models.

Window	Ufactor W/m ² ·K	SHGC	Tvis
Microperforated screen	1.337	0.26	0.398
Tubular shading structure (double)	1.789	0.606	0.707
Tubular shading structure (triple)	0.824	0.292	0.458
Expanded metal mesh	1.314	0.157	0.301

Table 6. Center of glass solar-optical and thermal properties of systems that were simulated.

ID	Window	Ufactor W/m ² - K	SHGC	Tvis
A	ASHRAE 90.1-2004 compliant window for Houston	4.46	0.26	0.14
B	ASHRAE 90.1-2004 compliant window for Chicago	3.06	0.24	0.18
C	ASHRAE 90.1-2010 compliant window for Houston	2.52	0.43	0.37
D	ASHRAE 90.1-2010 compliant window for Chicago	1.75	0.42	0.37
E1	Double-pane spectrally selective low-e	1.35	0.27	0.64
E2	E1 with indoor roller shade	1.28	0.16	0.09
E3	E1 with outdoor roller shade	1.09	0.05	0.07
F1	Triple-paned with suspended film and spectrally selective low-e	0.67	0.23	0.47
F2	F1 with indoor roller shade	0.64	0.18	0.06
F3	F1 with outdoor roller shade	0.60	0.04	0.05
G1	Microperforated screen	1.34	0.26	0.40
H1	Tubular shading structure (double)	1.79	0.61	0.71
H1T	Tublar shading structure (triple)	0.82	0.29	0.46
I1	Expanded metal mesh	1.31	0.16	0.30
G0	G1 without angular selective layer, Argon fill or low-e coating	2.69	0.73	0.81
G0g	G1 without angular selective layer or low-e coating	2.55	0.73	0.81
G0c	G1 without angular selective layer or Argon fill	1.62	0.37	0.64
G0gc	G1 without angular selective layer	1.35	0.37	0.64
H0	H1 without angular selective layer	2.69	0.70	0.78
H0g	H1 without angular selective layer or low-e coating	2.55	0.70	0.78
H0c	H1 without angular selective layer or Argon fill	1.97	0.62	0.73
H0gc	H1 without angular selective layer	1.76	0.62	0.73
I0	I1 without angular selective layer	2.06	0.63	0.71
I0g	I1 without angular selective layer or low-e coating	1.88	0.63	0.71
I0c	I1 without angular selective layer or Argon fill	1.32	0.28	0.56
I0gc	I1 without angular selective layer	1.08	0.28	0.56
H1G	G1 with tubular shading structure instead of microperforated screen	1.79	0.37	0.62
I1G	G1 with expanded metal mesh instead of microperforated screen	1.60	0.24	0.34

3. Results

South- and west-facing facades are the most likely to show significant energy impacts from window solar control. This section presents simulations results for perimeter zones of the South facade. Results for the West facade were similar.

3.1 Angular selective system performance vs. code compliant window

3.1.1 Annual energy consumption

Typical results are shown in Table 7 and Figure 7 for the three angle-selective systems and an unshaded window compliant with ASRHAE 90.1. Two of the angular-selective systems, the microperforated screen and the expanded metal mesh, perform consistently and significantly better than the benchmark unshaded windows, with savings of 30-50% energy use reduction, relative to the ASHRAE 90.1-2004 benchmark, usually achieved when daylighting controls are used. The expanded metal mesh system almost always performs the best of all three, reaching 47% savings for Chicago climate with WWR=0.45 and daylighting

controls. In its double-glazed configuration, the tubular shading structure has the highest energy consumption and the closest to the benchmark window, especially for Houston climate, with savings as low as -4% for WWR=0.60 and no daylighting controls. When coupled with daylighting controls, however, it can reach 32% savings, for Chicago and WWR=0.45. In its triple-glazed configuration, the performance of the tubular shading structure increases significantly, approaching and even surpassing (e.g., Chicago, no daylighting controls) the performance of the other two angular-selective layers.

It would be natural to expect that, because they involve occlusion of direct solar radiation, angular selective systems automatically provide less useful daylight than unshaded windows. Therefore, the fact that the spread between systems in Figure 7 is not significantly affected (in fact being even slightly greater in some cases) by the introduction of daylighting controls could seem, at first, surprising. The fact is, however, that the benchmark windows have much lower visible transmittance than the windows on which the angular selective systems are mounted. Visible transmittance at normal incidence is 0.14 for the Houston ASHRAE 90.1-2004 reference window, 0.37 for Chicago ASHRAE 90.1-2004 reference window, and 0.64, 0.73 and 0.56 for the microperforated screen, tubular shading device and expanded metal mesh windows without the angular selective layer. While the addition of the angular selective layer will reduce the transmittance of these windows, the starting point is substantially higher than the benchmark windows, and, for some sun angles, the net result could approach, or even surpass the benchmark light transmission.

Table 7. Annual source energy use intensity of angular selective systems and benchmark window for south-facing perimeter zones in Chicago and Houston, with and without daylighting controls.

Climate	Chicago					Houston				
Window	C	G1	H1	H1T	I1	A	G1	H1	H1T	I1
WWR	<i>No daylighting controls (MJ/m2-yr)</i>									
0.15	927	836	871	813	835	1270	1228	1265	1215	1204
0.3	1091	886	965	838	871	1343	1247	1341	1219	1185
0.45	1269	939	1076	870	908	1411	1262	1400	1219	1160
0.6	1269	998	1195	909	946	1411	1277	1462	1218	1140
	<i>Percentage savings compared to 90.1-2004 code baseline</i>									
0.15	0%	10%	6%	12%	10%	0%	3%	0%	4%	5%
0.3	0%	19%	12%	23%	20%	0%	7%	0%	9%	12%
0.45	0%	26%	15%	31%	28%	0%	11%	1%	14%	18%
0.6	0%	21%	6%	28%	25%	0%	9%	-4%	14%	19%
	<i>With daylighting controls (MJ/m2-yr)</i>									
0.15	729	682	775	757	700	1129	1046	1157	1150	1049
0.3	844	662	799	728	662	1129	982	1147	1093	938
0.45	995	684	863	718	671	1165	960	1159	1047	864
0.6	995	733	962	732	693	1165	964	1204	1026	831
	<i>Percentage savings compared to 90.1-2004 code baseline</i>									
0.15	21%	26%	16%	18%	24%	11%	18%	9%	9%	17%
0.3	23%	39%	27%	33%	39%	16%	27%	15%	19%	30%
0.45	22%	46%	32%	43%	47%	17%	32%	18%	26%	39%
0.6	22%	42%	24%	42%	45%	17%	32%	15%	27%	41%

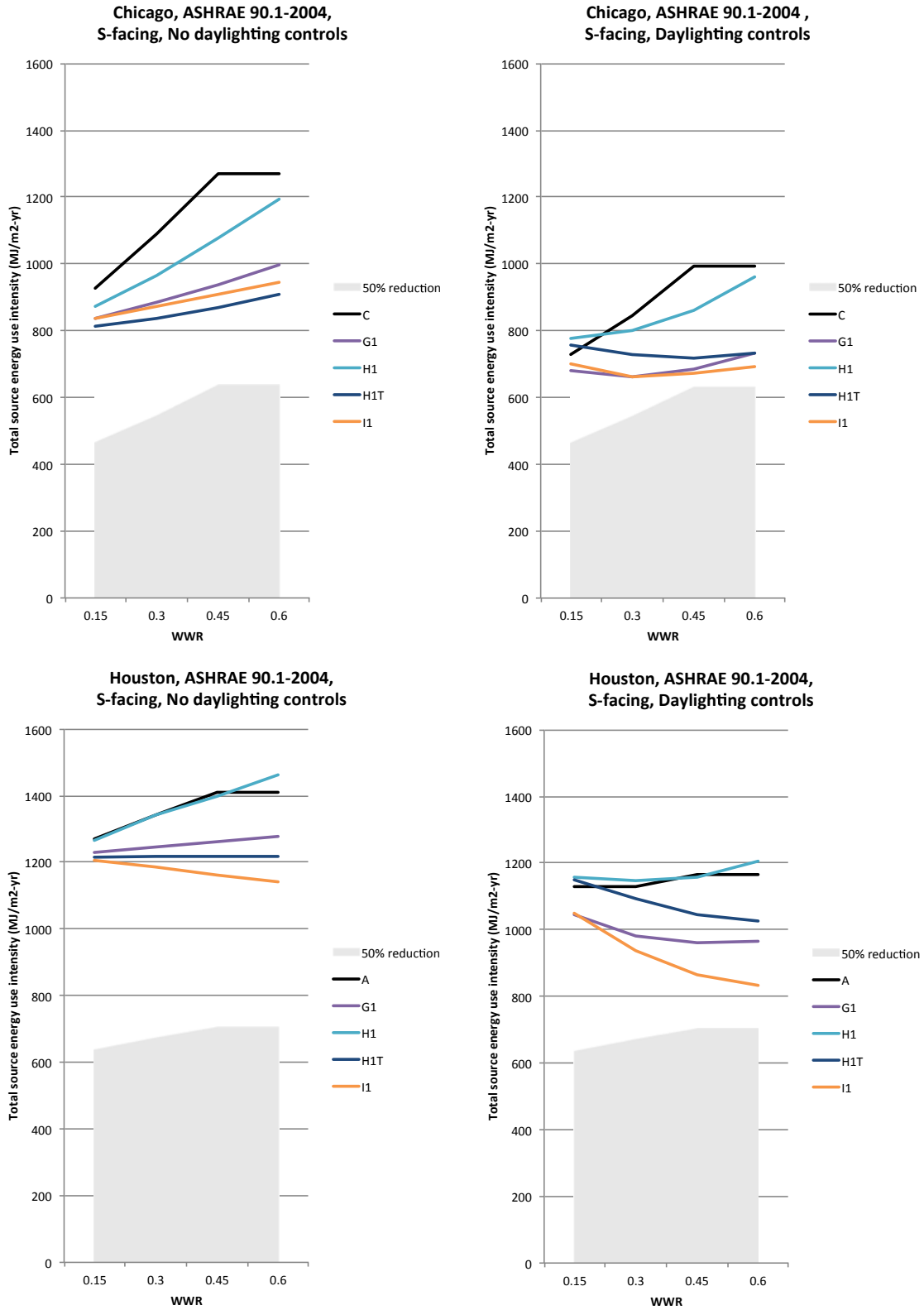


Figure 7. Annual source energy use intensity of angular selective systems and benchmark window for south-facing perimeter zones in Chicago and Houston, with and without daylighting controls.

3.1.2 Peak window heat gains

Figure 8 and Table 8 show typical peak window heat gains for both climates. The most striking feature of the plots is that the expanded metal mesh system performs consistently below 43 W/m^2 , indicating that angular selective systems have high potential to constrain peak window heat gains. A second striking feature is that, for the Houston climate, the tubular shading device, in its double-paned configuration, has even higher peak window heat gains than the reference window, only reaching the desired performance when WWR is 0.15. This could be taken to imply that angular selectivity alone cannot guarantee improved energy performance. The microperforated screen has peak gains below 43 W/m^2 for WWR equal to or less than 0.3; the tubular shading device, in its triple-paned configuration, has slightly better performance than the microperforated screen.

In facades exposed to the sun, peak window heat gains will be dominated by solar heat gains. Besides angular selectivity, another factor in solar heat gain control is the ability of the transparent parts of the glazing system to block the infrared part of the solar spectrum. The four angular selective system configurations are very different in this regard. The expanded metal mesh window, as well as one of the tubular shading structure configurations, has three glass layers, whereas the other two configurations have only two layers. Furthermore, the low-e coatings used in the windows that had microperforated screen, expanded metal mesh angular selective layers, as well as the triple-glazed tubular shading structure, are considerably more spectrally selective than the one used in the double-glazed tubular shading structure window (Figure 9). These differences probably play a significant role in explaining the relative performance of the four angular selective system configurations in terms of peak window heat gains.

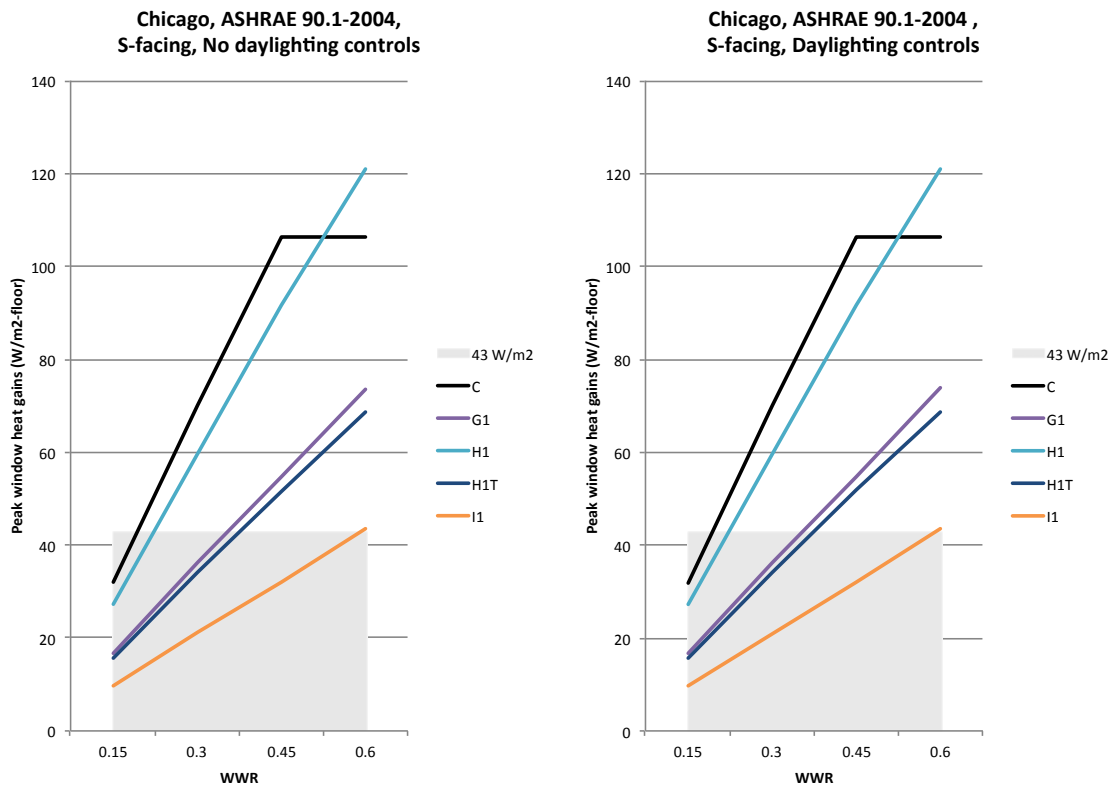


Figure 8. Peak window heat gains of angular selective systems and benchmark window for south-facing perimeter zones in Chicago and Houston without daylighting controls.

Table 8. Peak window heat gains of angular selective systems and benchmark window for south-facing perimeter zones in Chicago and Houston.

Climate	Chicago					Houston				
Window	C	G1	H1	H1T	I1	A	G1	H1	H1T	I1
WWR	<i>No daylighting controls (W/m2-floor)</i>									
0.15	31.9	16.6	27.3	15.6	9.7	22.9	16.8	24.8	14.0	9.3
0.3	70.1	36.1	59.6	34.0	21.1	49.5	36.3	53.4	29.8	20.2
0.45	106.4	54.7	91.6	51.6	32.1	75.6	55.4	81.6	45.4	30.8
0.6	106.4	73.6	120.9	68.6	43.5	75.6	72.2	105.5	58.3	40.3

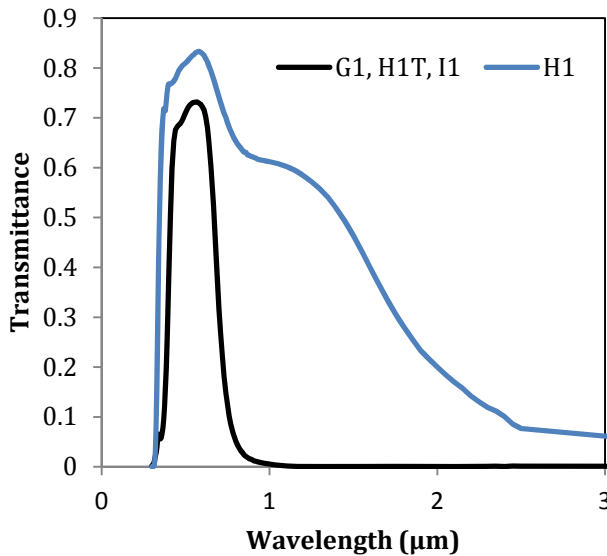


Figure 9. Spectral transmittance of coated glass in used in four angular-selective windows.

3.2 Angular selective system performance vs. “best-practice” windows

The ASHRAE 90.1 benchmark windows represent what could normally be used to comply with that standard, but do not represent, and might actually fall quite short of, what is currently best practice. To understand how angular selective windows perform versus the kind of windows that might be considered for high-performance buildings, we compared them to double- and triple-pane windows that had spectrally selective low emissivity coatings, in three configurations: unshaded, with interior shading (always down) and with exterior shading (always down). This third configuration provides the highest solar control, but requires the added maintenance of regular cleaning and is thus only suitable for low-rise buildings. Although always-down shading is not completely realistic, it can nonetheless provide a good basis for evaluating the effectiveness of the angular selective systems’ tradeoffs between solar control and admission of useful daylight.

3.2.1 Annual energy consumption

Figure 10 and Table 9 shows typical performance of the two-paned angular selective vs. double-pane spectrally selective low-e windows. Without daylighting controls, the shaded “best-practice” windows consistently show lower energy consumption than the unshaded configuration, with the lowest values for

the exterior-shaded window, which can be taken as evidence for the significance of cooling loads caused by window solar heat gains in both climates studied. In Chicago, the microperforated screen window performs slightly better than the interior-shaded “best-practice” windows. When daylighting controls are introduced, there is a marked decrease in energy use by the unshaded “best-practice” window. This is to be expected, since it admits the most daylight. The energy consumption with microperforated screen window is mostly between that of the unshaded and exterior-shaded “best-practice” window, indicating that even though angular selective systems admit more solar radiation, and hence higher solar heat gains, this effect can be offset by reductions in lighting energy use.

Figure 11 and Table 10 show the same comparison for triple-paned systems. Again, without daylighting controls, the lowest energy consumption is observed with exterior-shaded “best-practice” windows. The angular selective systems now show, for Chicago climate, similar performance to the unshaded or the interior-shaded “best” practice windows. With daylighting controls, the angular selective systems have performance between the unshaded and exterior-shaded “best-practice” windows, with the expanded metal mesh surpassing both for all but the highest WWR.

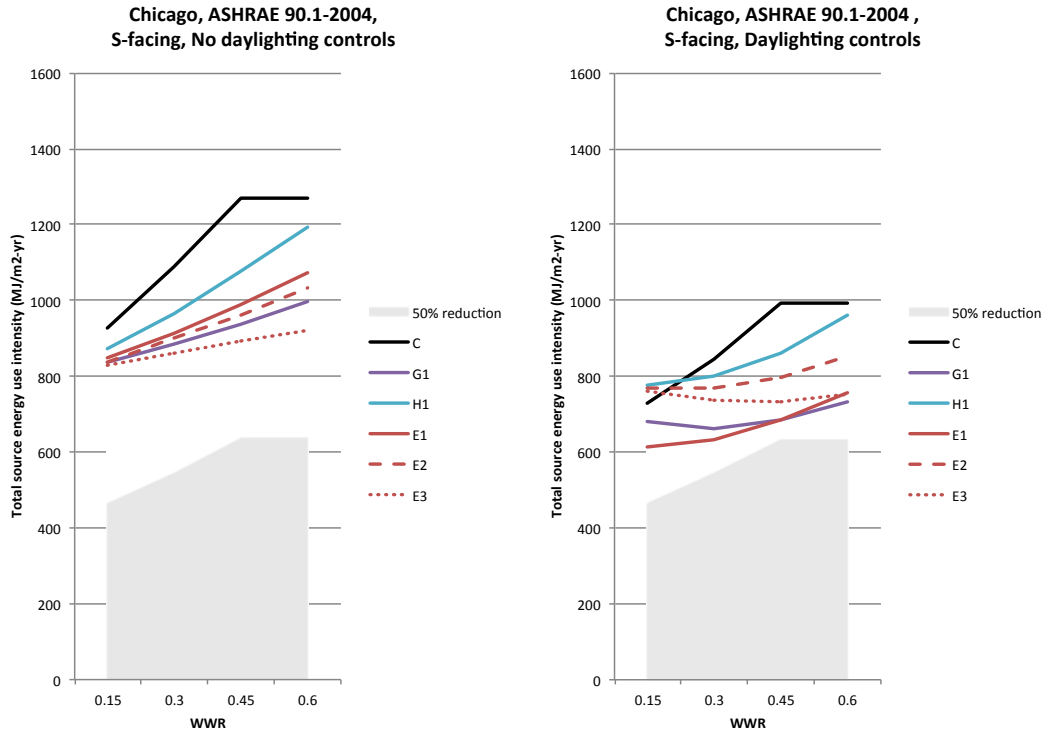


Figure 10. Annual source energy use intensity of double-paned angular selective system configurations and “best-practice” window for south-facing perimeter zones in Chicago, with and without daylighting controls.

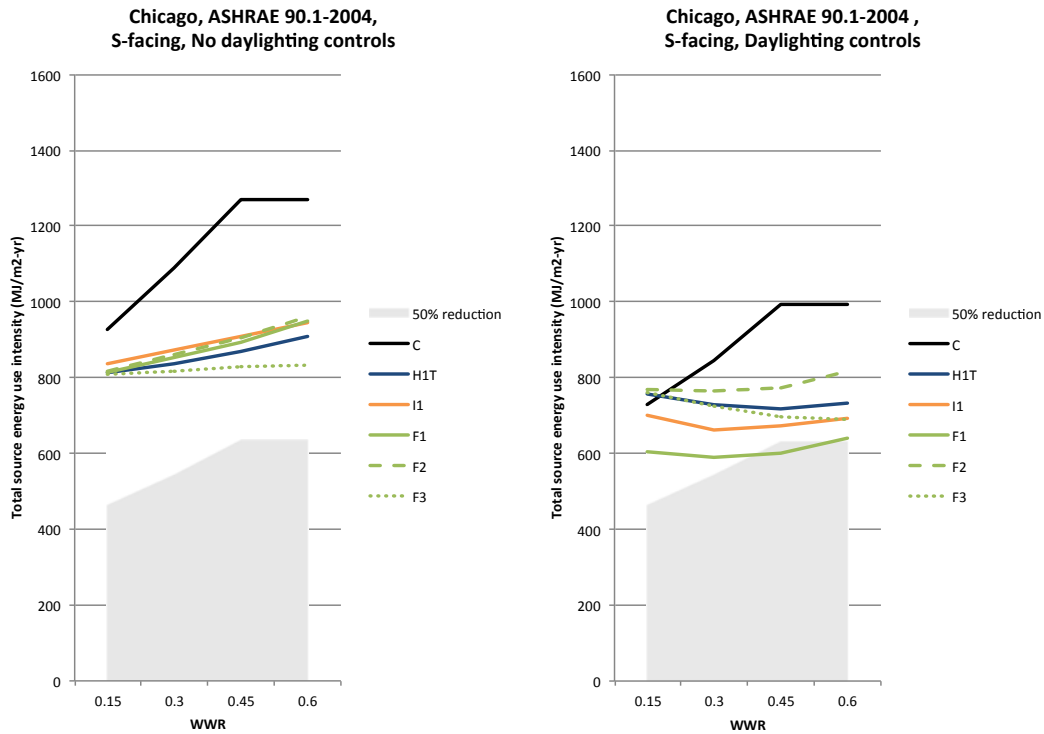


Figure 11. Annual source energy use intensity of triple-paned angular selective configurations and “best-practice” window for south-facing perimeter zones in Chicago, with and without daylighting controls.

Table 9. Annual source energy use intensity of double-paned angular selective system configurations and “best-practice” window for south-facing perimeter zones in Chicago and Houston, with and without daylighting controls.

Climate	Chicago					Houston				
Window	E1	E2	E3	G1	H1	E1	E2	E3	G1	H1
WWR	<i>No daylighting controls (MJ/m2-yr)</i>									
0.15	847	837	829	836	871	1254	1226	1189	1228	1265
0.3	912	900	861	886	965	1298	1248	1151	1247	1341
0.45	989	961	894	939	1076	1348	1257	1104	1262	1400
0.6	1073	1033	922	998	1195	1397	1273	1056	1277	1462
	<i>Percentage savings compared to 90.1-2004 code baseline</i>									
0.15	9%	10%	11%	10%	6%	1%	3%	6%	3%	0%
0.3	16%	18%	21%	19%	12%	3%	7%	14%	7%	0%
0.45	22%	24%	30%	26%	15%	4%	11%	22%	11%	1%
0.6	15%	19%	27%	21%	6%	1%	10%	25%	9%	-4%
	<i>With daylighting controls (MJ/m2-yr)</i>									
0.15	614	770	759	682	775	977	1148	1109	1046	1157
0.3	634	769	736	662	799	958	1102	1008	982	1147
0.45	683	795	733	684	863	983	1072	919	960	1159
0.6	755	855	751	733	962	1022	1071	858	964	1204
	<i>Percentage savings compared to 90.1-2004 code baseline</i>									
0.15	34%	17%	18%	26%	16%	23%	10%	13%	18%	9%
0.3	42%	30%	33%	39%	27%	29%	18%	25%	27%	15%
0.45	46%	37%	42%	46%	32%	30%	24%	35%	32%	18%
0.6	41%	33%	41%	42%	24%	28%	24%	39%	32%	15%

Table 10. Annual source energy use intensity of triple-paned angular selective system configurations and “best-practice” window for south-facing perimeter zones in Chicago and Houston, with and without daylighting controls.

Climate	Chicago					Houston				
Window	F1	F2	F3	H1T	I1	F1	F2	F3	H1T	I1
WWR	<i>No daylighting controls (MJ/m2-yr)</i>									
0.15	814	817	808	813	835	1232	1235	1184	1215	1204
0.3	853	861	818	838	871	1259	1271	1140	1219	1185
0.45	895	904	827	870	908	1290	1285	1089	1219	1160
0.6	948	963	831	909	946	1322	1314	1035	1218	1140
	<i>Percentage savings compared to 90.1-2004 code baseline</i>									
0.15	12%	12%	13%	12%	10%	3%	3%	7%	4%	5%
0.3	22%	21%	25%	23%	20%	6%	5%	15%	9%	12%
0.45	29%	29%	35%	31%	28%	9%	9%	23%	14%	18%
0.6	25%	24%	35%	28%	25%	6%	7%	27%	14%	19%
	<i>With daylighting controls (MJ/m2-yr)</i>									
0.15	603	768	759	757	700	983	1177	1129	1150	1049
0.3	590	765	723	728	662	946	1161	1031	1093	938
0.45	602	774	698	718	671	948	1144	945	1047	864
0.6	641	817	690	732	693	969	1159	874	1026	831
	<i>Percentage savings compared to 90.1-2004 code baseline</i>									
0.15	35%	17%	18%	18%	24%	23%	7%	11%	9%	17%
0.3	46%	30%	34%	33%	39%	30%	14%	23%	19%	30%
0.45	53%	39%	45%	43%	47%	33%	19%	33%	26%	39%
0.6	49%	36%	46%	42%	45%	31%	18%	38%	27%	41%

3.2.2 Peak window gains

In terms of peak window gains, typical results are shown in Figure 12 and Table 11, and confirm that angular selective windows have generally higher peak window heat gains than shaded “best-practice” windows, especially when compared with the exterior-shaded configuration.

Table 11. Peak window heat gains of angular selective systems and “best-practice” windows for south-facing perimeter zones in Chicago and Houston.

Climate	Chicago									
Window	E1	E2	E3	F1	F2	F3	G1	H1	H1T	I1
WWR	<i>No daylighting controls (W/m2-floor)</i>									
0.15	19.6	12.4	3.5	17.7	14.9	3.0	16.6	27.3	14.0	9.7
0.3	41.9	26.7	7.4	38.0	32.0	6.1	36.1	59.6	29.8	21.1
0.45	67.3	39.8	11.3	59.9	48.1	9.3	54.7	91.6	45.4	32.1
0.6	90.0	53.7	15.5	80.8	66.0	12.5	73.6	120.9	58.3	43.5
	<i>With daylighting controls (W/m2-floor)</i>									
0.15	19.6	12.4	3.6	17.8	15.0	3.0	16.6	27.3	14.0	9.7
0.3	42.0	26.9	7.5	38.1	32.4	6.3	36.2	59.6	29.9	21.1
0.45	67.3	40.4	11.4	60.1	48.8	9.5	54.8	91.7	45.7	32.2
0.6	90.1	54.5	15.8	81.1	66.9	12.8	73.9	120.9	58.7	43.5
Climate	Houston									
Window	E1	E2	E3	F1	F2	F3	G1	H1	H1T	I1
WWR	<i>No daylighting controls (W/m2-floor)</i>									
0.15	20.4	13.5	3.9	18.1	15.5	3.4	16.8	24.8	13.9	9.3
0.3	45.4	28.9	8.2	39.9	33.4	6.9	36.3	53.4	29.7	20.2
0.45	69.3	44.2	12.3	60.9	51.1	10.2	55.4	81.6	45.4	30.8
0.6	92.6	57.1	16.4	80.5	65.8	13.4	72.2	105.5	58.2	40.3
	<i>With daylighting controls (W/m2-floor)</i>									
0.15	20.4	13.6	3.9	18.1	15.7	3.4	16.8	24.9	14.0	9.3
0.3	45.6	29.3	8.2	40.1	33.8	6.9	36.5	53.5	29.9	20.3
0.45	69.6	44.8	12.3	61.2	51.7	10.3	55.6	81.8	45.6	31.0
0.6	92.9	57.9	16.7	80.9	66.7	13.7	72.5	105.8	58.6	40.6

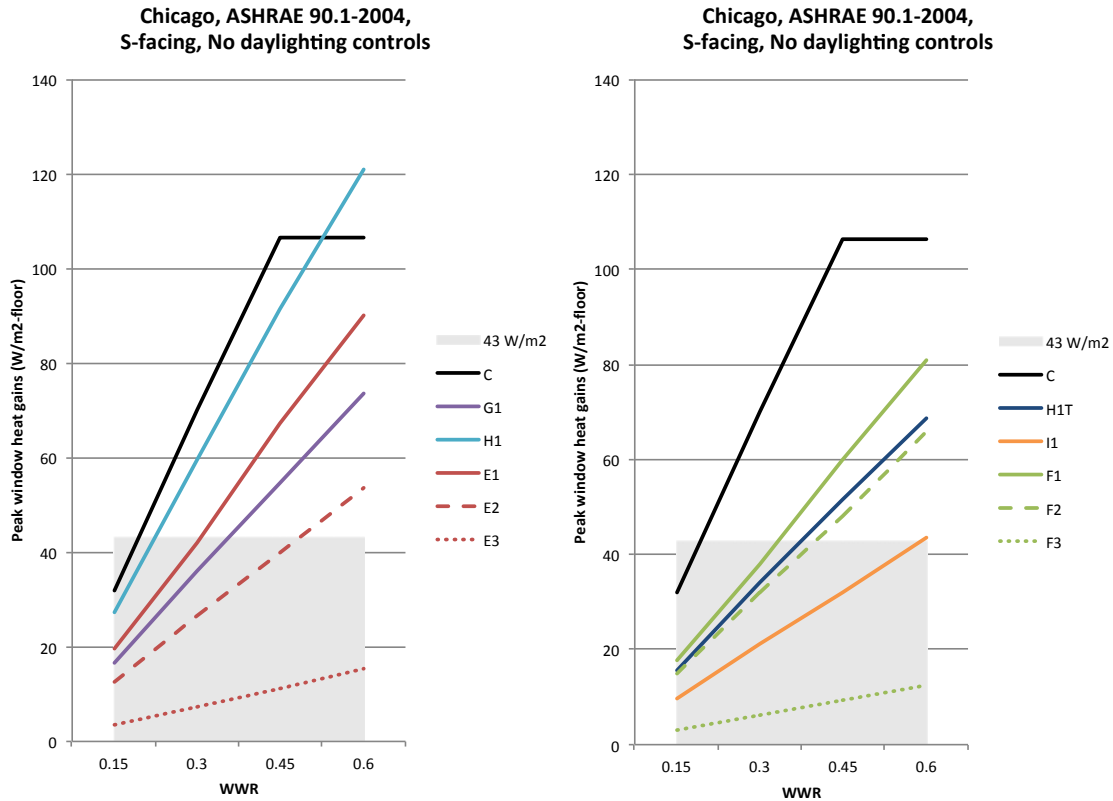


Figure 12. Peak window heat gains of angular selective systems and “best-practice” windows for south-facing perimeter zones in Chicago, without daylighting controls.

3.3 Performance of angular selective system components

It is natural to assume that the performance of the angular selective systems analyzed here is due not only to their angular selective layer, but also to the heat gain control provided by the multiple glass panes and low emissivity coatings. To understand the effect of each of these components, we simulated the performance of the systems without any angular selective layer, low-e coating or inert gas fill. We then simulated the systems again, adding each component one by one.

Typical results for annual energy consumption are shown in Figure 13. One of the most remarkable features is that the low-e glass coating ($e = 0.215$) for the tubular shading structure window provides a much smaller improvement than the spectrally selective low-e glass coating ($e = 0.018$) for the microperforated screen window. It seems reasonable to infer here that the tubular shading structure window would perform better with a more spectrally selective low-e coating.

3.4 Angular selective layer performance – annual energy use intensity

In order to fully isolate the effects of the angular selective layers, the behavior of each of the three layers was simulated with an identical IGU. For this purpose, the IGU construction of the microperforated screen window was used. Typical annual energy consumption is shown in Figure 14 and Table 12. Not only are the differences between the three systems somewhat narrower than in Figure 7, it is also noticeable that, for the Chicago climate, the microperforated screen system now leads to the lowest energy consumption by a small margin.

The plots also show that the angular selective layers perform more similarly to each other when there are no daylighting controls. When such controls are introduced, there is a noticeable increase in the energy consumption of the tubular daylighting structure, relative to the other two systems. A possible cause for this distinction becomes apparent when one examines the visible transmittance of each window as a function of incidence angle (Figure 15). Although the tubular shading structure has highest transmittance at normal incidence, it falls off rapidly for off-normal incidence, whereas the other two systems show broader angular transmittance.

Table 12. Annual source energy use intensity of angular selective system layers with identical IGU for south-facing perimeter zones in Chicago and Houston, with and without daylighting controls.

Climate	Chicago				Houston			
Window	C	G1	H1G	I1G	A	G1	H1G	I1G
WWR	<i>No daylighting controls (MJ/m2-yr)</i>							
0.15	927	836	867	857	1270	1228	1252	1221
0.3	1091	886	964	918	1343	1247	1323	1224
0.45	1269	939	1067	988	1411	1262	1376	1229
0.6	1269	998	1184	1056	1411	1277	1427	1233
	<i>Percentage savings compared to 90.1-2004 code baseline</i>							
0.15	0%	10%	6%	8%	0%	3%	1%	4%
0.3	0%	19%	12%	16%	0%	7%	1%	9%
0.45	0%	26%	16%	22%	0%	11%	2%	13%
0.6	0%	21%	7%	17%	0%	9%	-1%	13%
	<i>With daylighting controls (MJ/m2-yr)</i>							
0.15	729	682	785	710	1129	1046	1162	1048
0.3	844	662	811	701	1129	982	1155	965
0.45	995	684	876	739	1165	960	1156	927
0.6	995	733	970	793	1165	964	1193	920
	<i>Percentage savings compared to 90.1-2004 code baseline</i>							
0.15	21%	26%	15%	23%	11%	18%	9%	17%
0.3	23%	39%	26%	36%	16%	27%	14%	28%
0.45	22%	46%	31%	42%	17%	32%	18%	34%
0.6	22%	42%	24%	38%	17%	32%	15%	35%

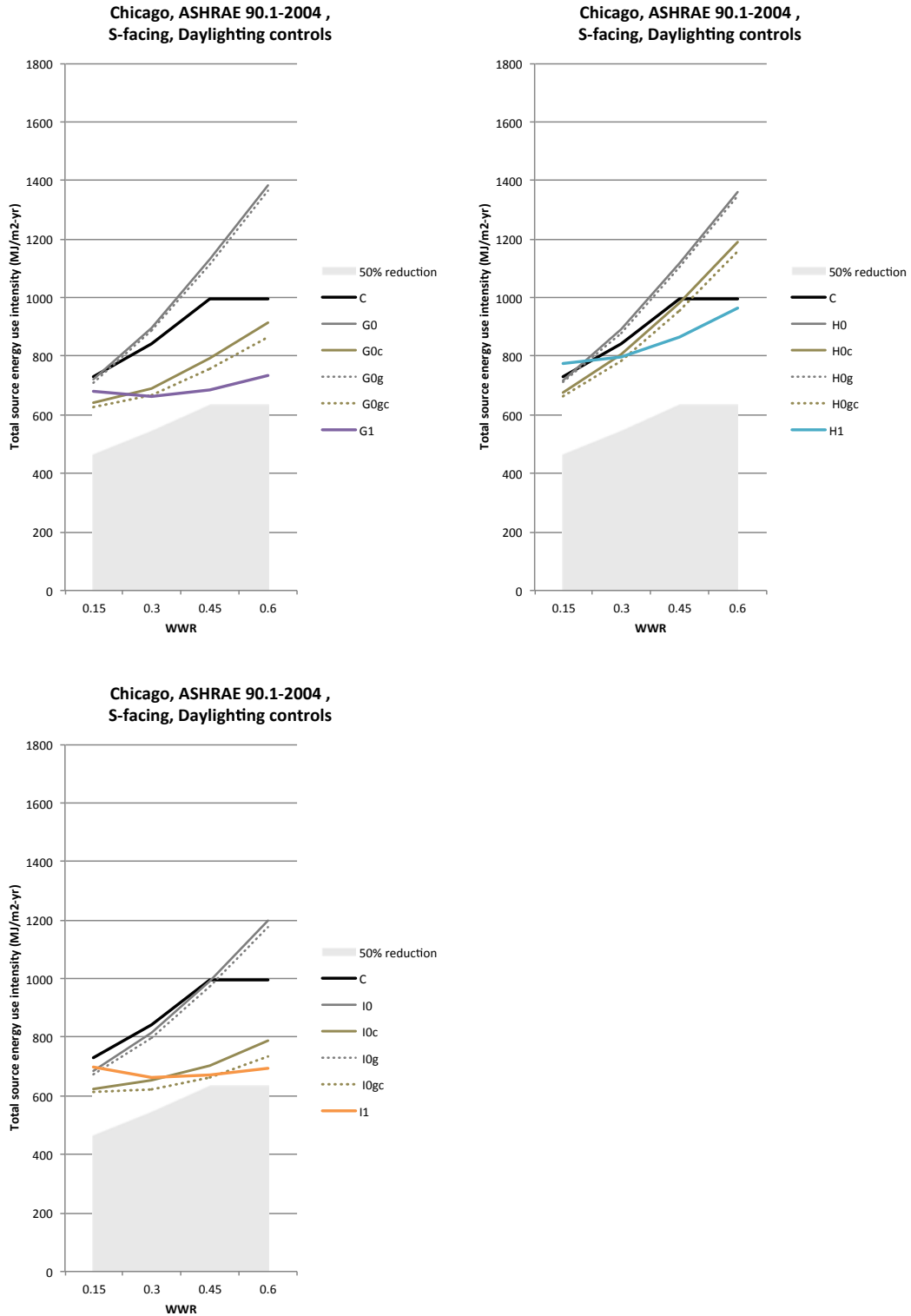


Figure 13. Annual source energy use intensity of angular selective system components for south-facing perimeter zones in Chicago, with daylighting controls.

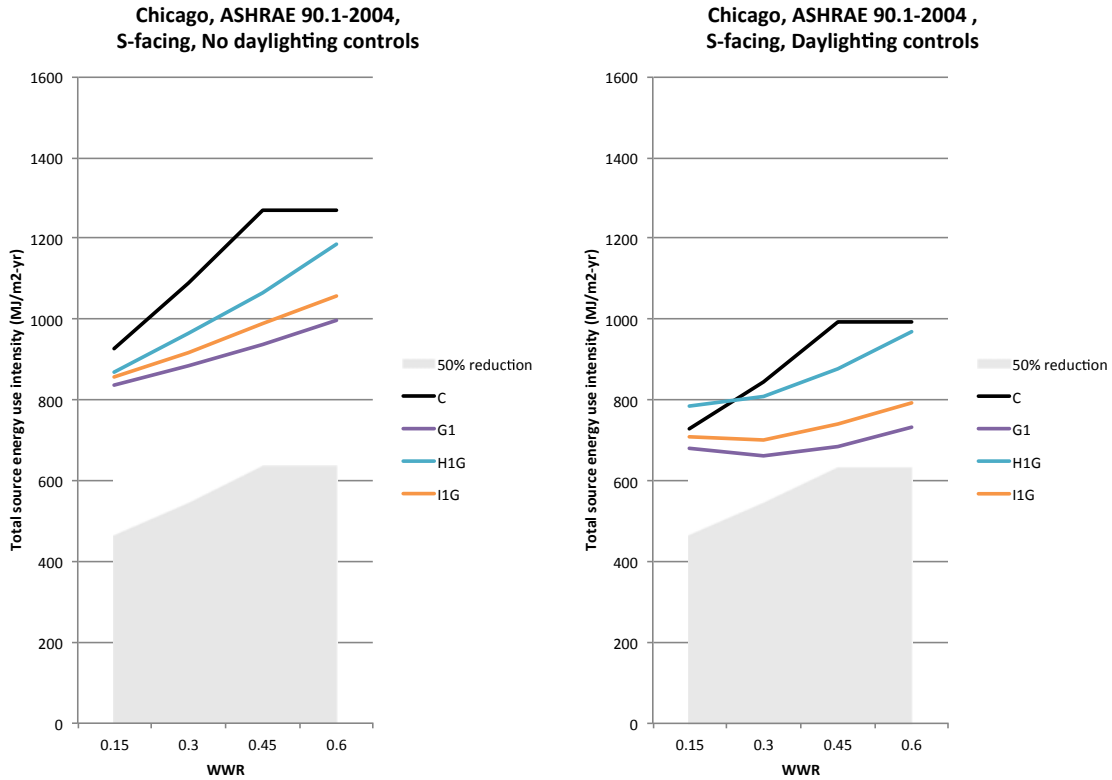


Figure 14. Annual source energy use intensity of angular selective system layers with identical IGU for south-facing perimeter zones in Chicago, with and without daylighting controls.

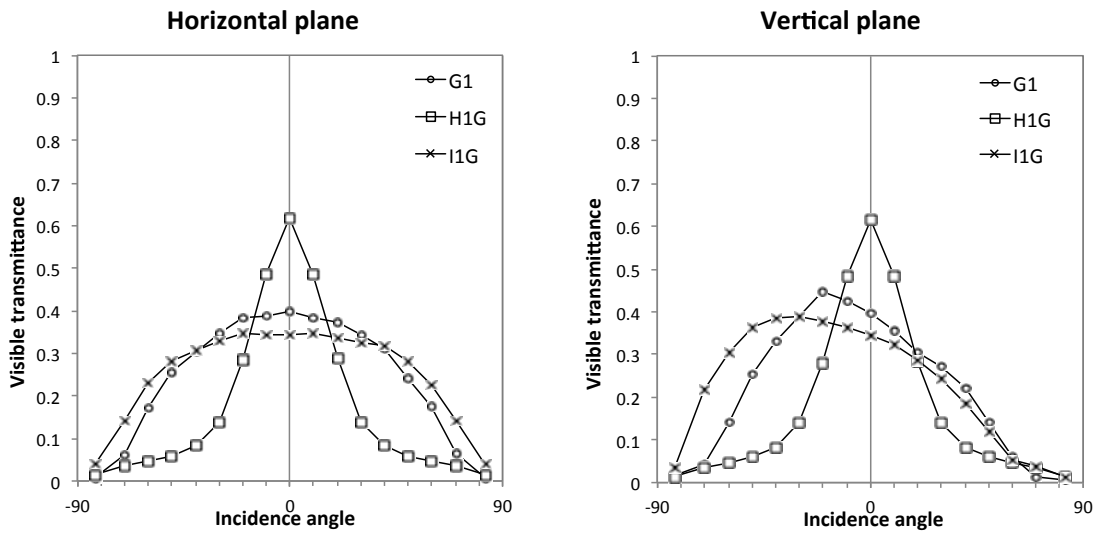


Figure 15. Directional-hemispherical visible transmittance vs. angle of incidence across vertical and horizontal planes for angular selective system layers with identical IGU.

3.5 Angular selective layer performance – hourly zone loads and window heat gains

To further understand the differences in performance between the three types of angular selective layer, we also analyzed hourly results for identical-IGU simulations. So that performance could be easily compared across different times of the day and year, a batch of simulations was conducted in which the HVAC setpoint was held constant at 21°C throughout the simulation period.

Figures 16 and 17 show hourly predicted cooling and heating loads for south-facing perimeter zones in Chicago, with WWR=0.45 and with no daylighting controls. These plots indicate that the differences in system performance are due to the cumulative effect over the whole year (or substantial parts of the year) of relatively small differences, rather than large differences localized in certain parts of the day or year. Cooling loads are the lowest for the expanded metal mesh window, but not very far from the microperforated screen. The tubular shading structure has the highest cooling loads, noticeably higher than the other systems during the middle of the day in the summer and fall. As for heating loads, they are quite similar between the three systems, with the microperforated screen having a slight advantage. In terms of their annual distribution, cooling loads tend to concentrate around the middle of the day (10 AM to 2 PM), particularly in the fall and (slightly less so) in the winter. Heating loads are concentrated around the fall and winter night time.

Figure 18 shows hourly zone heat gains from windows. Here there is a clear difference between the tubular shading structure and the other two angular selective layers, with the former exhibiting distinctly higher heat gains. The annual distribution is similar to cooling loads, with highest gains concentrated in the middle of the day primarily during fall and winter. This makes sense when considering that these are the periods during which the sun is lowest in the sky and therefore the density of incident radiation on the window will be highest.

It might seem surprising, at first, that the difference in window heat gains between the tubular shading structure and the other two systems does not reflect itself as clearly in the magnitude of cooling loads. Window heat gains result in cooling loads by directly or indirectly heating the air inside the building. The cooling system responds by cooling the air in the building when thermostats detect temperatures above the cooling setpoint. A significant component of window heat gains, and especially so during times of high cooling loads, is due to transmitted solar radiation. This radiation, however, does not instantly increase the air temperature inside the building, its effect being mediated by the heating of the interior surfaces of the building, which then transfer heat to the air. This process can slow down the impact of direct solar heat gains on cooling loads, and could play a significant part in the spreading of the differences between the systems, in terms of hourly cooling load, over longer periods of time.

To have a quantitative measure of the contribution of each system to improving or worsening HVAC loads, we used the following metric. For each hour of the year, if there was a heating load, window heat gains were counted as beneficial, and losses as detrimental. If instead there was a cooling load, window heat gains were counted as detrimental, and losses as beneficial. Adding the beneficial and detrimental contributions for all hours of the year yielded the net benefit of the system. Although this metric does not take into account the delayed effect of window heat transfer on HVAC loads, it has the advantage of being able to account for small, cumulative differences between systems throughout the day and year.

Table 13 shows the results for each of the three angular selective systems. One can see that the major disadvantage of the tubular shading structure relative to the other two systems is high cumulative heat gains while cooling. Given its lower light transmission away from normal incidence, it is possible that its higher thermal conductance (1.79 W/m²K) also plays a role here. It might seem surprising that this doesn't seem to affect the expanded metal mesh window (with a conductance of 1.60 W/m²K), but this window has much lower visible and solar absorptance (Figure 19). It is also interesting to note that the microperforated screen has significantly lower heat loss while heating, which would be due to its lower thermal conductance (1.34

W/m²K). Solar heat gains are unlikely to be a significant factor here since most heating loads occur during night time.

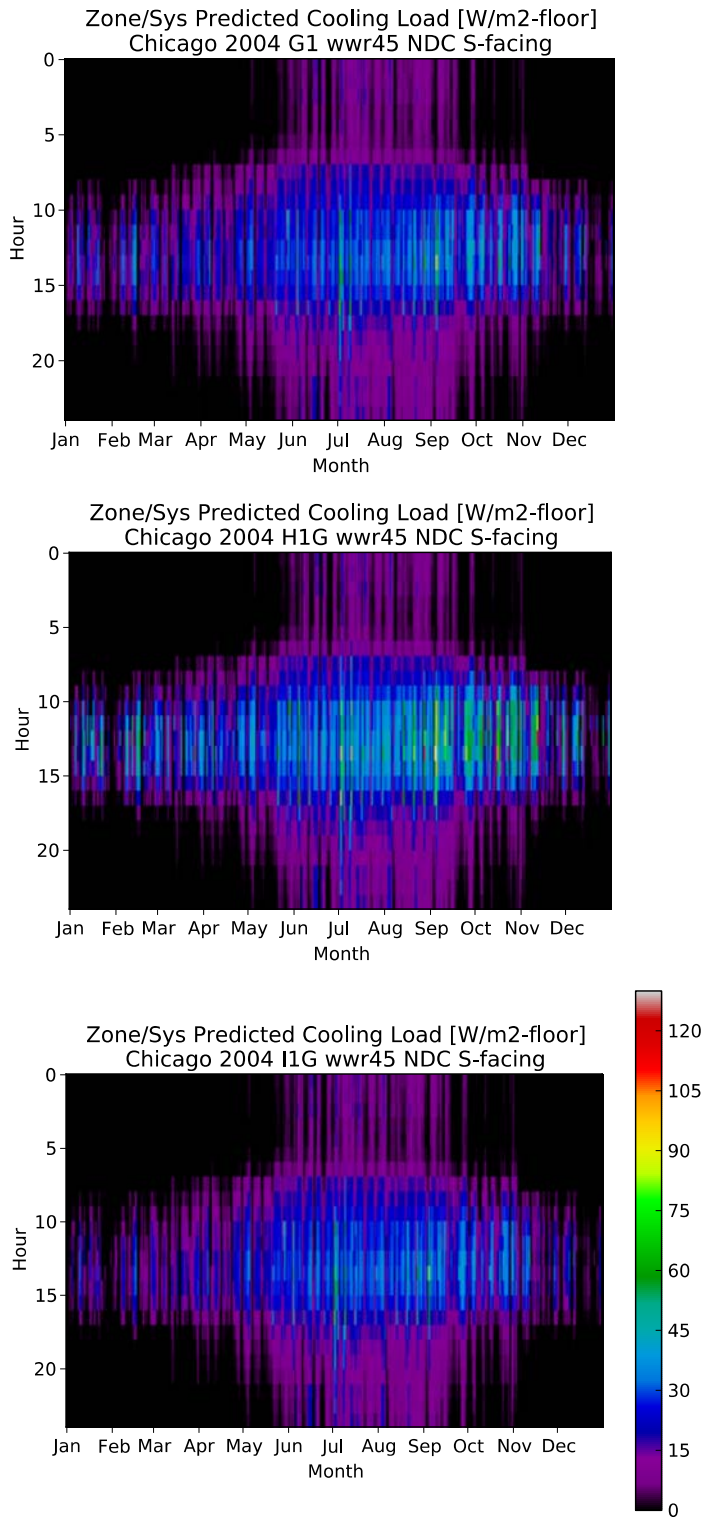


Figure 16. Hourly predicted cooling load with three different angular selective layers in identical IGUs, for south-facing perimeter zones in Chicago and WWR=0.45.

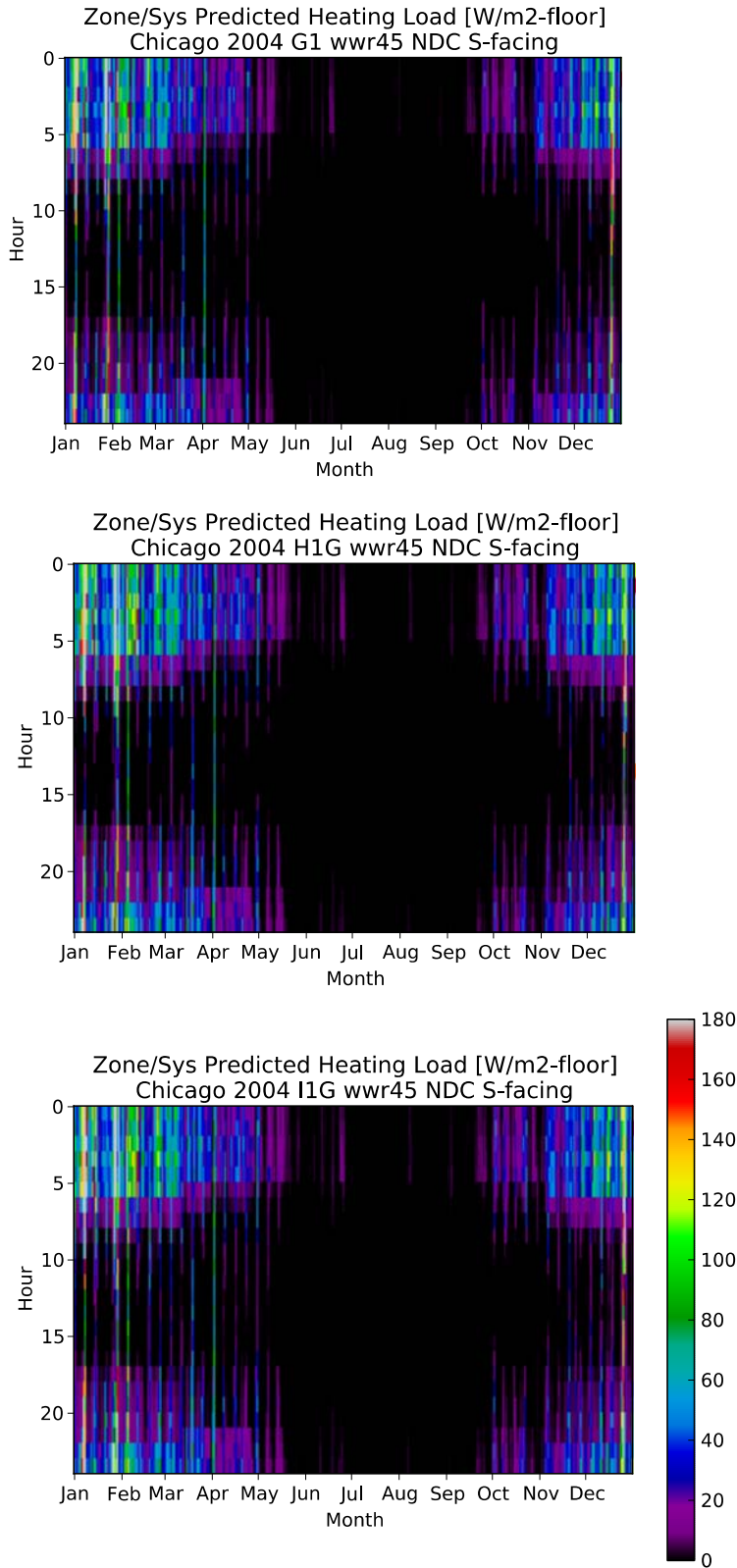


Figure 17. Hourly predicted cooling load with three different angular selective layers in identical IGUs, for south-facing perimeter zones in Chicago and WWR=0.45.

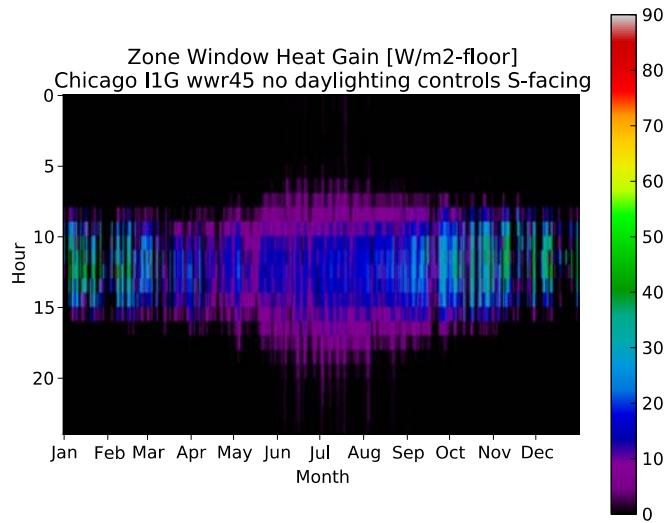
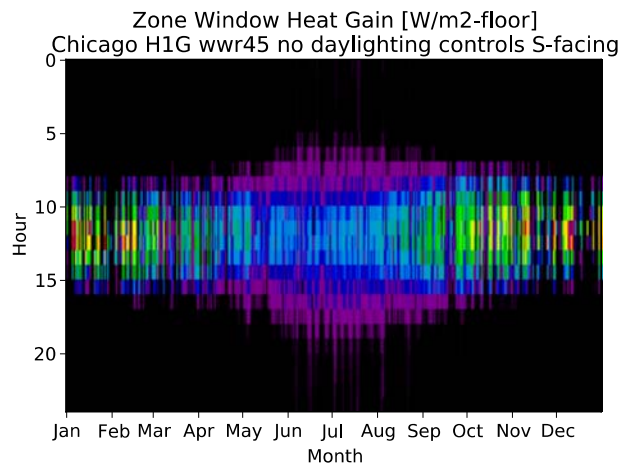
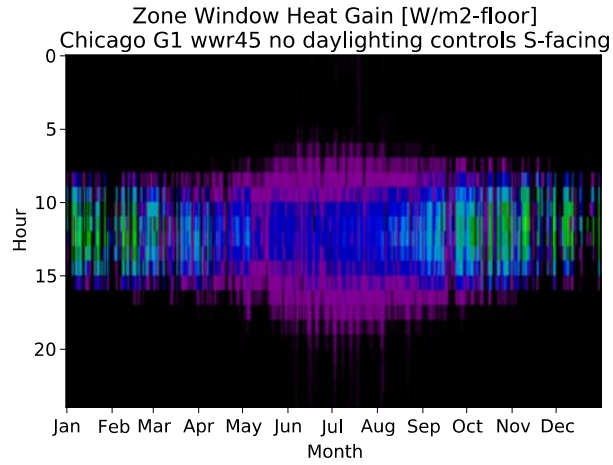


Figure 18. Hourly window heat gains with three different angular selective layers in identical IGUs, for south-facing perimeter zones in Chicago and WWR=0.45.

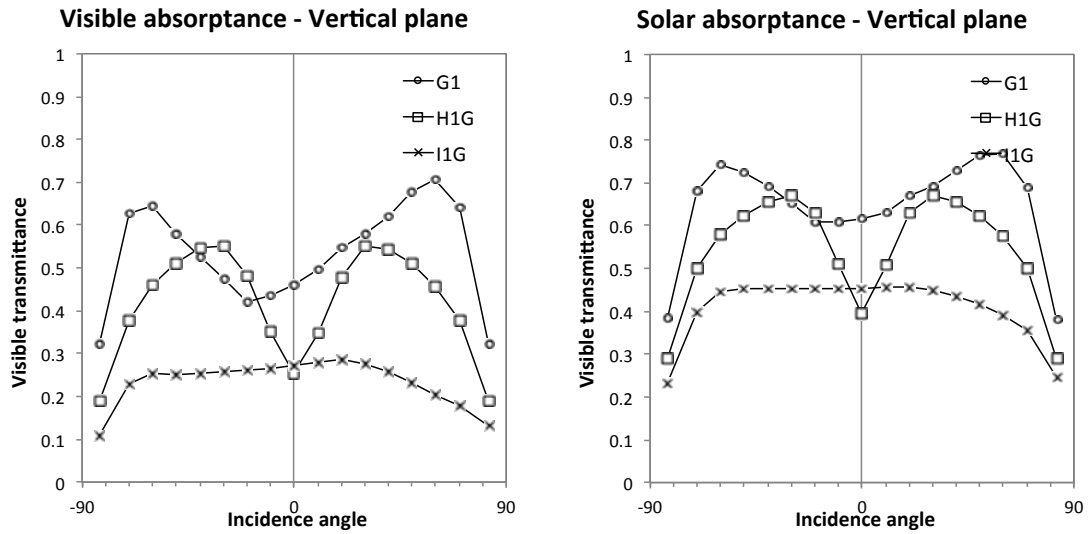


Figure 19. Directional-hemispherical visible and solar absorptance vs. angle of incidence across vertical plane for angular selective system layers with identical IGU.

Table 13. Contributions to HVAC loads of the three different angular selective layers in identical IGUs, for south-facing perimeter zones in Chicago and WWR=0.45.

		Microperforated screen (G1)	Tubular shading structure (H1G)	Expanded metal mesh (I1G)
Heat gain (MJ/m ² -floor)	while heating	9	7	9
	while cooling	143	207	118
Heat loss (MJ/m ² -floor)	while heating	93	136	132
	while cooling	21	26	25
Total		-206	-310	-216

3.6 Angular selective layer performance – shading, glare and view

Angular selective shading systems have the potential to reduce the need for deployable shading. Operable shading, when left down for extended periods, can increase lighting energy use due to a lowering of daylight availability. To understand this potential, we examined the bi-directional visible transmission coefficients for straight-through transmission of each system’s BSDF. Figure 20 shows the directions for which straight-through transmission is less than 2%, with superimposed sunpaths for vertical fenestration facing south, and 42°N latitude (approximately the latitude of Chicago).

It is striking that the tubular shading structure practically never admits direct sunlight. Potential for glare from direct solar visibility is therefore practically zero, for this orientation. There could still be potential for glare due to diffused light. Conversely, view to the exterior will be significantly reduced by this system, possibly limiting its widespread application to mostly non-view fenestration.

For the microperforated screen, the sun will be shaded all day for approximately 25% of the year (May 6 to August 6). For the expanded metal mesh, this is the case for 38% of the year (April 13 to August 29). This means that, during those periods, and for this orientation, there will be no need to deploy operable shading due to glare from direct visibility of the sun. During the rest of the year, the sun will not be shaded during parts of or the whole day, which brings high potential for glare and likelihood of occupants deploying operable shading. This greater openness, however, will allow better views of the exterior when operable shading is not deployed.

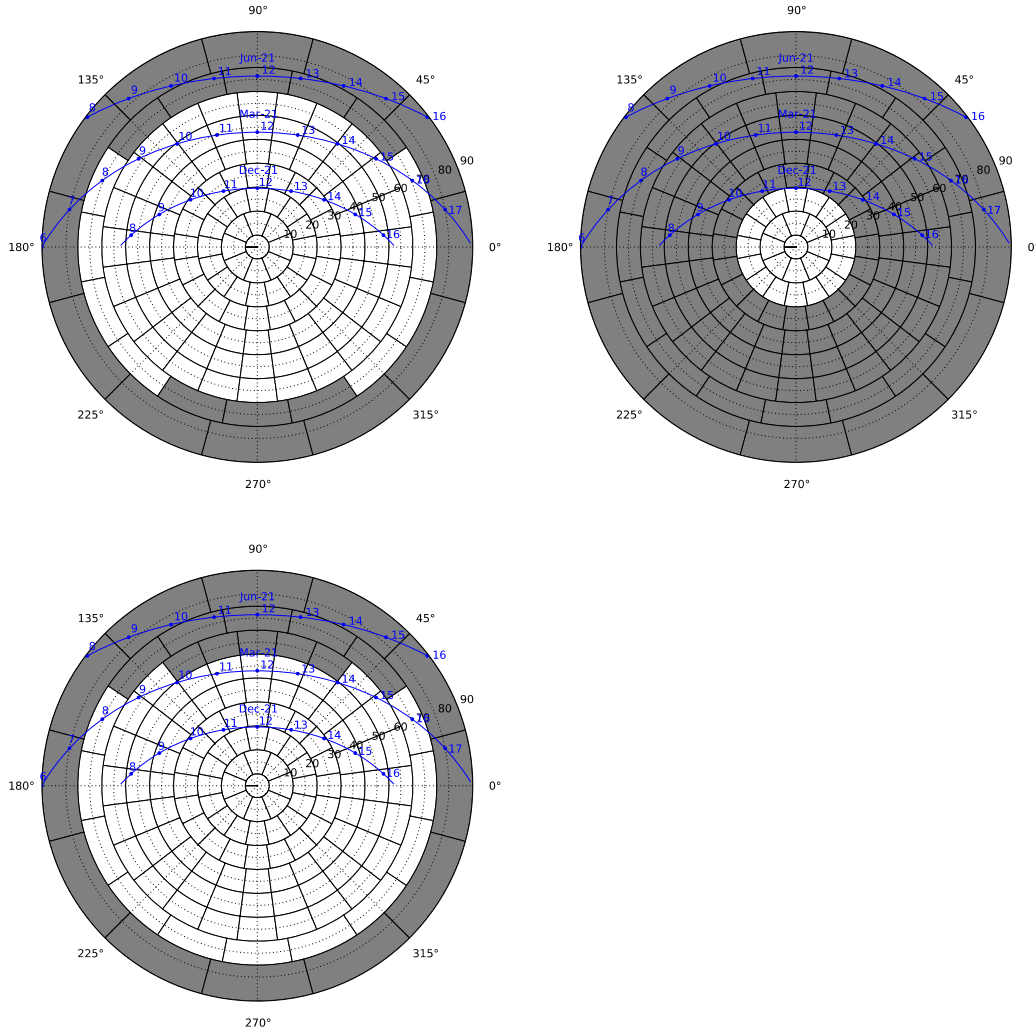


Figure 20. Shading diagrams for the three different angular selective layers in identical IGUs, facing south at latitude 42° N (Chicago): microperforated screen (G1) (*top left*), tubular shading structure (H1G) (*top right*), expanded metal mesh (I1G) (*bottom left*). Shaded sectors represent visible straight-through transmission of 2% or less.

4. Analysis

4.1 Do commercially-available angular selective systems provide value compared to IGUs without an angular selective component?

Overall, the simulation results presented in the previous section strongly suggest that angular selective windows can provide significant energy savings in the perimeter zones of buildings, relative to non-angular selective windows. This was evidently the case when compared to ASHRAE 90.1-compliant windows (Figure 7), but also noticeable for the angular selective window IGUs with the angular selective layer removed (Figures 13 and 14). There was a wide range in performance, but improvements were observed whether the IGU was relatively low-performing, as was the case of the pyrolytic-coated IGU of the tubular shading structure double-paned window, or highly insulating, such as the IGUs of the expanded metal mesh or the tubular shading structure triple-paned window, which were triple-glazed with spectrally selective low-e coatings.

When placed in an IGU with a highly spectrally selective low-e coating, angular selective systems can perform very well when compared to shaded or unshaded high-performance windows, especially if the angular selective layer does not excessively increase IGU thermal conductivity.

4.2 How much energy savings can angular selective systems be expected to provide?

Savings can vary substantially according to climate, orientation, window-to-wall ratio, angular selective window and presence of daylighting controls. For south-facing zones in Chicago climate (Table 7), savings could be as high as 28% and 47% without and with daylighting controls, respectively, for expanded metal mesh windows with WWR = 0.45. For the microperforated screen window, which has an IGU that is perhaps more representative of commonly-installed windows, savings are still quite significant: 26% and 46% without and with daylighting controls, respectively, and WWR=0.45. For these two systems, savings were mostly 20% or above, which shows a significant savings potential. For Houston climate, savings were generally lower, but reaching the vicinity of 40% for the expanded metal mesh window with WWR of 0.45 and above, when coupled with daylighting controls. Results for west-facing zones were in the same order of magnitude.

4.3 Is it worth it to improve existing angular selective systems? How?

The facts that angular selective systems are practically maintenance-free (they can be mounted between an IGU's glass panes or inside a retrofit add-on such as storm windows) and permanently in place (i.e. they don't depend on occupant operation), mean that the energy savings they provide have the potential to be highly reliable and therefore applicable to a broad swath of the building inventory.

There appears to be significant improvement potential beyond the performance of currently-existing systems. It is noticeable, when comparing Figure 16 and Figure 18, that even the better-performing angular selective systems still exhibit significant window heat gains during times of peak cooling loads. Reducing gains during these periods would most probably have a positive impact in energy performance, especially if admission of useful daylight is not excessively compromised.

5. Conclusions

Static, angular selective shading systems offer a potentially low-cost option to significantly reduce window heat gains and block direct sun, while permitting daylight and views to the outdoors. This type of system shows significant potential to contribute towards net-zero energy goals in both new and retrofit construction.

Simulations for Chicago and Houston climates show significant potential reductions in perimeter zone energy use, with the best commercially-available system reaching 28% and 47% savings, relative to ASHRAE 90.1-2004 and respectively without and with daylighting controls, on south facades in Chicago with WWR=0.45, while constraining peak window heat gains to under 43 W/m²-floor. Results suggest that it is possible that existing systems can be improved to more consistently achieve 30-50% savings.

During this study, a few factors have been identified as having significant impact on the performance of angular selective systems: level of angular selectivity, spectral selectivity of low-e coatings and thermal conductance of the angle-selective layer. If the system excessively constrains the direct admission of sunlight, energy savings from daylighting controls start to diminish, as well as view to the exterior. Glare from direct visibility of the sun might be significantly reduced, however. Energy use and peak solar gain performance is best when the IGU has highly spectrally selective low-e coatings. Finally, the benefits of angular selectivity may be negated if the angular selective excessively increases the window's thermal conductivity. While other factors that were not studied here in detail may also significantly impact on performance, the factors identified in this paper should be taken into consideration in the improvement of existing angular selective systems or development of new ones.

Acknowledgements

We would like to thank and acknowledge our LBNL colleagues for their contribution to this research: Charlie Curcija, Christian Kohler, David Appelfeld, Howdy Goudey, and Robin Mitchell.

This work was supported by the Assistant Secretary for Energy Efficiency and Renewable Energy, Office of Building Technology, State and Community Programs, Office of Building Research and Standards of the U.S. Department of Energy under Contract No. DE-AC02-05CH11231 and by the California Energy Commission through its Public Interest Energy Research (PIER) Program on behalf of the citizens of California.

References

- [1] Reppel, J., Edmonds, I.R., 1998, *Angle-selective glazing for radiant heat control in buildings: theory*, Solar Energy 62(3):245-253.
- [2] Smith, G.B., Dligatch, S., Sullivan, R., Hutchins, M.G., 1998, *Thin film angular selective glazing*, Solar Energy 62(3):229-244.
- [3] Sullivan, R., Beltran, L., Lee, E.S., Rubin, M., Selkowitz, S.E., *Energy and daylight performance of angular selective glazings*, Proceedings of the ASHRAE/DOE/BTECC Conference, Thermal Performance of the Exterior Envelopes of Buildings VII, Clearwater Beach, Florida, December 7-11, 1998.
- [4] Haves, P., Linden, P.F., Carrilho da Graça, G., 2004, *Use of simulation in the design of a large, naturally ventilated office building*, Building Serv. Eng. Res. Technol. 25(3):211-221.
- [5] Rubins, A.I., Collins, B.L., Tibbott, R.L. 1978, *Window blinds as a potential energy saver - A case study* (NBS Building Science Series 112), Washington, DC, USA. Department of Commerce, National Bureau of Standards.
- [6] Jonsson, J.C., Rubin, M.D., Nilsson, A.M., Jonsson, A., Roos, A., 2009, *Optical characterization of fritted glass for architectural applications*, Optical Materials 31(6):949-958.
- [7] Klems, J.H., 1994, *A new method for predicting the solar heat gain of complex fenestration systems. I. Overview and derivation of the matrix layer calculation*. ASHRAE Transactions, V. 100, Pt. 1.

- [8] Klems, J.H., 1994, *A new method for predicting the solar heat gain of complex fenestration systems. II. Detailed description of the matrix layer calculation*. ASHRAE Transactions, V. 100, Pt. 1.
- [9] Nilsson, A.M., Jonsson, J.C., 2010, *Light-scattering properties of a Venetian blind slat used for daylighting applications*, Solar Energy 84(12):2103-2111.
- [10] Grobe, L.O., Wittkopf, S., Apian-Bennowitz, P., Jonsson, J.C., Rubin, M., *Experimental validation of bidirectional reflection and transmission distribution measurements of specular and scattering materials*, Proc. SPIE 7725 (2010); doi:10.1117/12.854011.
- [11] Saxena M., Ward, G., Perry, T., Heschong, L., Higa, R., 2010, *Dynamic Radiance – Predicting annual daylighting with variable fenestration optics using BSDFs*, Fourth National Conference of IBPSA-USA, New York City, New York, August 11 – 13, 2010.
- [12] Ward, G., Mistrick, R., Lee, E.S., McNeil, A. and Jonsson, J., 2011, *Simulating the Daylight Performance of Complex Fenestration Systems Using Bidirectional Scattering Distribution Functions within Radiance*, Leukos 7(4).
- [13] McNeil, A., Lee, E. S., 2012, *A validation of the Radiance three-phase simulation method for modelling annual daylight performance of optically complex fenestration systems*. Journal of Building Performance Simulation, 1-14, doi:10.1080/19401493.2012.671852.
- [14] U.S. Department of Energy, *EnergyPlus Engineering Reference*, October 13, 2011.
- [15] Windows and Daylighting Group, 2006, *Window 6.1/Therm 6.1 Research version user manual*, LBNL-941, September 2006.
- [16] McNeil, A., Jonsson, C.J., Appelfeld, D., Ward, G., Lee, E.S., 2013, *A validation of a ray-tracing tool used to generate bi-directional scattering distribution functions for complex fenestration systems*, Solar Energy 98 (2013) 404-414.
- [17] Appelfeld, D., McNeil, A., Svendsen, S., 2012, *An hourly based performance comparison of an integrated micro-structural perforated shading screen with standard shading systems*, Energy and Buildings 50(July 2012):166:176.
- [18] Department of Energy, 2012, *Commercial prototype building models*, https://www.energycodes.gov/development/commercial/90.1_models, accessed on Sep. 21, 2012.